

Galactic Longitude Dependent Galactic Model Parameters

S. Bilir ^{a,*}, S. Karaali ^a, S. Ak ^a, E. Yaz ^a and E. Hamzaoglu ^b

^a*Istanbul University, Faculty of Sciences, Department of Astronomy and Space Sciences, 34119 University, Istanbul, Turkey*

^b*Beykent University, Faculty of Engineering and Architecture, Department of Computer Engineering, Beykent 34500, Istanbul, Turkey*

Abstract

We present the Galactic model parameters for thin disc estimated by Sloan Digital Sky Survey (*SDSS*) data of 14 940 stars with apparent magnitudes $16 < g_o \leq 21$ in six intermediate latitude fields in the first Galactic quadrant. Star/galaxy separation was performed by using the *SDSS* photometric pipeline and the isodensity contours in the $(g - r)_0 - (r - i)_0$ two colour diagram. The separation of thin disc stars is carried out by the bimodal distribution of stars in the $(g - r)_o$ histogram, and the absolute magnitudes were evaluated by a procedure presented in the literature (Bilir, Karaali & Tunçel, 2005). Exponential density law fits better to the derived density functions for the absolute magnitude intervals $8 < M(g) \leq 9$ and $11 < M(g) \leq 12$, whereas sech/sech² laws are more appropriate for absolute magnitude intervals $9 < M(g) \leq 10$ and $10 < M(g) \leq 11$. We showed that the scaleheight and scalelength are Galactic longitude dependent. The average values and ranges of the scaleheight and the scalelength are $\langle H \rangle = 220$ pc ($196 \leq H \leq 234$ pc) and $\langle h \rangle = 1900$ pc ($1561 \leq h \leq 2280$ pc) respectively. This result would be useful to explain different numerical values claimed for those parameters obtained by different authors for the fields in different directions of the Galaxy.

Key words: Galaxy: disk, Galaxy: fundamental parameters, Galaxy: structure, stars: luminosity function, mass function

* corresponding author.

Email address: sbilir@istanbul.edu.tr (S. Bilir).

1 Introduction

The study of Galactic models and parameters have long history. Bahcall & Soneira (1980) fitted observations to two-component Galactic model, namely disc and halo, while Gilmore & Reid (1983) successfully fit their observations to a Galactic model introducing a third component, i.e. the thick disc. It should be noted that the third component was a rediscovery of the “Intermediate Population II” first described in the Vatican Proceedings review of O’Connell (1958). Due to their importance, Galactic models have been primary concern and research topic for many research centers: As they can be used as a tool in order to understand the formation and evolution of the Galaxy.

Different research groups have been using different methods to determine Galactic model parameters (Table 1). For example, Chen et al. (2001) and Siegel et al. (2002) give 6.5-13 and 6-10 per cent, respectively, for the relative local space density of the thick disc. However, we think that an appropriate procedure would lead us to expect a smaller range and/or a unique value with a small error.

In the previous studies (Karaali, Bilir & Hamzaoglu, 2004, hereafter KBH; Bilir, Karaali & Gilmore, 2006, hereafter BKG) we estimated Galactic model parameters for stars of different Galactic populations and absolute magnitude intervals and we found that the range of these models are rather small relative to the ones appeared in the literature. It gives the indication that this procedure refines the Galactic model parameters. However such a result may not be considered in the model estimation due to the contamination introduced by the other populations. In the present study we estimated the Galactic model parameters only for the thin disc and our previous results are confirmed. Also, we showed (Section 5.1) that the contamination of the thick disc is rather small. Additionally we discussed the dependence of the Galactic model parameters on the Galactic longitude. For this, we used the homogeneous *SDSS* data for stars in six intermediate Galactic latitude fields in the first Galactic quadrant. The range of the latitudes of the fields is comparatively small, $41^\circ \leq b \leq 52^\circ$, whereas the longitudes of the fields lie between 5° and 83° . Hence, any significant difference between the values of a given Galactic model parameters derived for stars in the same absolute magnitude interval for two fields could be attributed to the effect of the Galactic longitude, under the condition that our data are not contaminated by other populations, i.e. thick disc. The sample stars are at distances less than $r \sim 2$ kpc relative to the Sun, and as stated above, the thick disc contamination is rather small. Thus, we can say that Galactic model parameters are longitude dependent, at least for the six fields investigated in the present study.

In Section 2 we describe the data and reductions, in Section 3 we introduce

the density laws adopted in the present study. Section 4 provides the absolute magnitude determination, and the evaluation of the density functions for thin disc of six fields. In Section 5 we estimate the Galactic model parameters, and the final conclusion is presented in Section 6.

2 Data and reductions

The data were taken from *SDSS*, Data Release 3 (DR3), on the WEB¹ of six fields with intermediate Galactic latitude ($41^\circ \leq b \leq 52^\circ$) in the first Galactic quadrant (Table 2). *SDSS* magnitudes u , g , r , i , and z were used for totally 113 380 stars in six fields equal in size (10 deg²) except Field F6 (20 deg²), down to the limiting magnitude of $g_0 = 21$. The mean $E(B - V)$ colour excess for each field is less than 0.06 except for the Field F1, $E(B - V) = 0.10$. The $E(B - V)$ colour excesses were individually evaluated for each sample source making use of the maps of Schlegel, Finkbeiner & Davis (1998) through *SDSS* query server and this was reduced to total absorption A_V via equation (1).

$$A_V = 3.1E(B - V). \quad (1)$$

In order to determine total absorptions, A_m , for the *SDSS* bands, we used A_m/A_V data given by Fan (1999), i.e. 1.593, 1.199, 0.858, 0.639 and 0.459 for $m=u, g, r, i$ and z , respectively. Thus, the de-reddened magnitudes, with subscript 0, are

$$u_0 = u - A_u, \quad g_0 = g - A_g, \quad r_0 = r - A_r, \quad i_0 = i - A_i, \quad z_0 = z - A_z. \quad (2)$$

All the colours and magnitudes mentioned hereafter will be de-reddened ones.

According to Chen et al. (2001), the distribution of stars in the apparent magnitude-colour diagram, $g_0 - (g - r)_0$, can be classified as follows. The blue stars in the range $15 < g_0 < 18$ are dominated by thick-disc stars with turn-off at $(g - r)_0 \sim 0.33$, and for $g_0 > 18$ the Galactic halo stars, with turn-off at $(g - r)_0 \sim 0.2$, become significant. Red stars, $(g - r)_0 \sim 1.3$, are dominated by thin disc stars at all apparent magnitudes.

However, the apparent magnitude-colour diagram and the three two-colour diagrams for all objects (due shortage of space large amount of data not presented here) indicate that the stellar distributions are contaminated by extragalactic objects as claimed by Chen et al. (2001). Distinction between star/galaxy was obtained using command `probPSFmag` given in DR3 WEB

¹ <http://www.sdss.org/dr3/access/index.html>

page. There 1 or 0 is designated for the probability of object being a star or galaxy. Needless to say, separation of 1 or 0 strongly depends on seeing and sky brightness. Apart from the above mentioned work, simulations of Fan (1999) were carefully adopted in order to remove the extragalactic objects in our field. This is similar to the procedure of Jurić et al. (2005) who defined locus points and drew several isodensity contours in the $(g-r)_0$ - $(r-i)_0$ two colour diagrams and rejected stars on the contours at distances larger than 0.3 mag relative to the corresponding locus (Fig. 1).

The colour-magnitude diagram g_0 - $(g-r)_0$ for the final sample (stars) are given in Fig. 2. The limiting magnitude for the survey stars in Fig. 2 can be read off as $g_0 = 22$. However, the colour and magnitude errors for fainter magnitudes are larger, i.e. $(\sigma_{u-g} = 0.26, \sigma_{g-r} = 0.04, \sigma_{r-i} = 0.04, \sigma_{i-z} = 0.07)$ for $g_0 = 21$, and $(\sigma_{u-g} = 0.75, \sigma_{g-r} = 0.06, \sigma_{r-i} = 0.05, \sigma_{i-z} = 0.08)$ for $g_0 = 22$ hence we adopted $g_0 = 21$ as the limiting magnitude in our work for the evaluation of more reliable Galactic model parameters.

3 Density laws

Disc structures are usually parametrized in cylindrical coordinates by radial and vertical exponentials,

$$D_i(x, z) = n_i \exp(-z/H_i) \exp(-(x - R_0)/h_i), \quad (3)$$

where z is the distance from the Galactic plane, x is the planar distance from the Galactic centre, R_0 is the solar distance from the Galactic centre (8.6 kpc, Buser, Rong & Karaali (1998)), H_i and h_i are the scaleheight and scalelength, respectively, and n_i is the normalized density at the solar radius. The suffix i takes the values 1 and 2 as long as the thin and thick discs are considered. A similar form uses the sech^2 or sech function to parameterize the vertical distribution of the thin disc. As the sech function is the sum of the two exponentials, the scaleheight corresponding to the sech^2 and sech has to be multiplied by 1.08504 and 1.65745, respectively (see Appendix A and Phleps et al. (2000)), for its reduction to the equivalent exponential appendix.

Here, we compare the density laws and the derived densities only for the thin disc. Hence, only the corresponding laws and parameters are considered.

4 Absolute magnitudes, distances and density functions for late-type thin-disc stars

Contrary to the thick disc and halo stars which overlap in the apparent magnitude–colour diagram, the position of the late-type thin disc stars is very conspicuous in the diagram. In fact, the $(g - r)_0$ histogram for all stars in six fields show a bimodal distribution, one at $(g - r)_0 \sim 0.45$ and another one at $(g - r)_0 \sim 1.35$ (Fig. 3). The Gaussian fit shows that $(g - r)_0 = 1.10$ can be adopted as the border separating the late-type thin disc stars from the thick disc and halo couple. Thus, totally 14 940 stars with $(g - r)_0 \geq 1.10$ included into our programme as thin-disc stars (details are given in Section 5.1).

The absolute magnitudes of the programme stars were evaluated using the following calibration (Bilir, Karaali & Tunçel, 2005)

$$M(g) = 5.791(\pm 0.023)(g - r)_0 + 1.242(\pm 0.012)(r - i)_0 + 1.412(\pm 0.021)(\sigma = 0.05). \quad (4)$$

Combination of the absolute magnitude $M(g)$ and the apparent magnitude g_0 of a star gives its distance r relative to the Sun, i.e.,

$$[g - M(g)]_0 = 5 \log r - 5. \quad (5)$$

For the six fields, the logarithmic space density functions were evaluated for different absolute magnitude intervals however, only the one for the Field F4 is given in Table 3 (due to shortage of space), but all of them are shown in Fig. 4 as $D^* = \log D + 10$, where $D = N/\Delta V_{1,2}$; $\Delta V_{1,2} = (\pi/180)^2(A/3)(r_2^3 - r_1^3)$; A denotes the size of the field (deg^2) in question; r_1 and r_2 denote the lower and upper limiting distance of the volume $\Delta V_{1,2}$; N is the number of stars; $r^* = [(r_1^3 + r_2^3)/2]^{1/3}$ is the centroid distance of the volume $\Delta V_{1,2}$; and $z^* = r^* \sin(b)$, b being the Galactic latitude of the field center in question. The thick horizontal lines in Table 3 correspond to the limiting distance of completeness, z_l , which are calculated from the following equations:

$$[g - M(g)]_0 = 5 \log r_l - 5, \quad (6)$$

$$z_l = r_l \sin(b), \quad (7)$$

where g_0 is the limiting apparent magnitude (16 and 21, for the bright and faint stars, respectively), r_l is the limiting distance of completeness, and $M(g)$ is the corresponding absolute magnitude in the interval (M_1, M_2) .

5 Galactic longitude dependent Galactic model parameters

5.1 Estimation of Galactic model parameters by comparison of the observation-based density functions with different density laws

A χ^2 method was employed to fit the analytical density laws given in Section 3 for thin disc to the observation-based space densities with the additional constraint of producing local densities consistent with those derived from Hipparcos (Jahreiss & Wielen, 1997). This procedure was applied in our previous papers (KBH, BKG).

One must be certain that our space density functions should belong to stars of the thin disc before discussing the Galactic model parameters, evaluated by the comparison mentioned above. Our strong argument is about the distance of stars relative to the Sun: All stars are at distances less than $r \sim 2$ kpc, and most of them at distances shorter than 1.5 kpc (Fig. 4). 25 stars with distances $2 < r \leq 3.5$ kpc relative to the Sun (Table 3) are beyond the limiting distance of completeness which are not included into the statistics. However, fitting the observed data to the Galactic model for the field F4, as example, in Fig. 5 shows that there is a slight excess in the observational based number of stars in the distances near to the Galactic plane $1 < z \leq 1.5$ kpc. This means some contamination of the thick disc. Comparison of the observational based data for the field F4 with the Galactic model of Chen et al. (2001) for two extreme scaleheights and solar normalizations of the thick disc, i.e. $H = 600$ pc; $n_2/n_1 = 12$ per cent, and $H = 1000$ pc; $n_2/n_1 = 3$ per cent (Figs. 6 and 7) confirms this suggestion. Now, the question is to find out the amount of this contamination. The locus of stars estimated in our work for absolute magnitude intervals $8 < M(g) \leq 9$ and $11 < M(g) \leq 12$ are below the model curve of thin disc of Chen et al. (2001). Whereas for the intervals $9 < M(g) \leq 10$ and $10 < M(g) \leq 11$ there is an excess in number of stars for the distance intervals $z < 500$ pc relative to the model curve thin disc, indicating some contamination of the thick disc in our work. We reduced the excess number of observed stars in Fig. 6 (Figs. 6 and 7 are rather similar) such as to fit to the predicted ones for the thin disc in the Galactic model of Chen et al. (2001), and we re-estimated the Galactic model parameters for the field F4. The contamination of the thick disc in number of stars are 7, 14, and 16 per cent for the absolute magnitude intervals $8 < M(g) \leq 9$, $9 < M(g) \leq 10$, and $10 < M(g) \leq 11$, respectively. The differences between three sets of parameters, for the previous Galactic model and the one with re-estimated parameters are as follows: $\Delta n^* = (0.01, 0.00, 0.01)$, $\Delta H = (3, 5, 1)$ pc, $\Delta h = (60, 563, 27)$ pc for the absolute magnitude intervals in the order given above. These small amounts show that the contamination of the thick disc is rather small. The Galactic model with the re-estimated parameters

mentioned above fit to the observational based data (Fig. 8). Hence our results stated in the following sections can be attributed to as the properties of the thin disc.

It turned out that the exponential law fitted better for the brightest and faintest intervals, i.e. $8 < M(g) \leq 9$ and $11 < M(g) \leq 12$, whereas sech and sech² laws are appropriate for the intermediate intervals, i.e. $9 < M(g) \leq 10$ and $10 < M(g) \leq 11$, respectively. The numerical values for χ^2_{min} given in Table 4, of the columns 7 and 12 substantiate our suggestion.

The resulting Galactic model parameters are summarized in Table 4. The scaleheights for the sech and sech² laws are reduced in accordance with the exponential law by multiplying them with 1.65745 and 1.08504, respectively. Hence, the symbol H in Table 4 corresponds to the exponential law. It is seen that the parameters are absolute magnitude-dependent for six fields. For example, the scaleheight is shorter for the brightest and faintest intervals with respect to one for the intermediate intervals. Also, the scalelength changes from one absolute magnitude interval to the other, without following any rule or pattern.

Here we present a question: Is it possible to claim that the scales substantially change with Galactic longitude? The answer of this question can be obtained by fitting one disc model to the stars in a given absolute magnitude range for six fields at the same time. Fig. 9 compares the derived logarithmic space densities for the absolute magnitude interval $10 < M(g) \leq 11$ for six fields with the thin disc model of Chen et al. (2001). The corresponding scaleheight and scalelength of the model are $H=330$ pc and $h=2250$ pc, respectively. The agreement between the derived data and the model is rather low. Additionally, the standard deviations are large and the resulting solar space densities for six fields are different than the Hipparcos (Jahreiss & Wielen, 1997) one for the same absolute magnitude interval (Table 5). The disagreement mentioned above indicates that the claim related to the scales change with Galactic longitude is valid.

All error estimates in Table 4 were obtained by changing Galactic model parameters until an increase or decrease by 1 in χ^2 was achieved (Phleps et al., 2000). The parameters were tested against the luminosity function given in Table 4 (last column) and Fig. 10, where $\varphi^*(M)$ is the local space density for thin disc. The absence of the local space densities for thick disc and halo, which is limited to ~ 10 per cent of the total local space density, did not affect the smooth agreement between the luminosity function and the derived from Hipparcos data (Jahreiss & Wielen, 1997).

5.2 Dependence of the scaleheight and scalelength on the galactic longitude

An interesting result can be deduced from Table 4 where the dependence of the scaleheight (H), and scalelength (h), on the Galactic longitude (l), for each absolute magnitude interval is seen. In fact, Table 6, Fig. 11 and Fig. 12 show that H and h change linearly from one interval to the other i.e.

$$H = a_1 l + a_0, \quad (8)$$

$$h = b_1 l + b_0, \quad (9)$$

where the coefficients a_i and b_i ($i=1, 2$) are given in Table 7. The correlation is higher for the scaleheight than for the scalelength and the correlation coefficient for the scaleheight decreases from the bright absolute magnitude intervals to the faint ones, contrary to the one for scalelength. The correlation coefficient of H for the interval $11 < M(g) \leq 12$ is rather small, $R^2 = 0.09$, and the slope coefficient is negative, i.e. $a_1 = -0.158$, in contradiction with the others.

The dependence of the scaleheight and scalelength on the Galactic longitude has so far not been claimed anywhere in the literature. Hence it is a novelty.

6 Summary and discussion

In the present study, we used the homogeneous *SDSS* data for stars in six intermediate Galactic latitude fields in the first Galactic quadrant and derived Galactic model parameters for the thin disc. Star/galaxy separation was performed by utilizing the command `probPSFmag` in DR3 WEB page to provide each object's probability of being a star in each filter. As the quality of this separation strongly depends on the seeing and sky brightness, we adopted also the simulation of Fan (1999) in order to remove the extragalactic objects from our sample. This is similar to the procedure of Jurić et al. (2005) who define locus points and draw several isodensity contours in the $(g-r)_0 - (r-i)_0$ two colour diagram and reject stars on the contours at distances larger than 0.3 mag relative to the corresponding locus. Thin disc stars were separated from the thick disc and halo stars by the bimodal distribution of stars in the $(g-r)_0$ histogram. Comparison of the observational based space density functions with the Galactic model of Chen et al. (2001) revealed that there is a slight contamination, i.e. 7, 14, and 16 per cent for the absolute magnitude intervals $8 < M(g) \leq 9$, $9 < M(g) \leq 10$, and $10 < M(g) \leq 11$, respectively, of the thick disc which does not affect the resulting Galactic model parameters

considerably. Thus, we obtained a sample of 14 940 thin disc stars with apparent magnitude $16 < g_0 \leq 21$ and colour indice $(g - r)_0 \geq 1.10$. The absolute magnitudes were evaluated according to the new calibration appeared in one of our papers (Bilir, Karaali & Tunçel, 2005).

The range of the Galactic model parameters estimated for different absolute magnitude intervals, i.e. $8 < M(g) \leq 9$, $9 < M(g) \leq 10$, $10 < M(g) \leq 11$ and $11 < M(g) \leq 12$, is rather small relative to the ones appeared in the literature. Hence, our previous results (KBH and BKG) are confirmed.

As in our previous works, we added the constraint of producing densities at the solar radius consistent with those derived from *Hipparcos* (Jahreiss & Wielen, 1997), and showed that the exponential density law fits better to the density functions for the brightest and faintest intervals, $8 < M(g) \leq 9$ and $11 < M(g) \leq 12$, whereas sech and sech^2 are more suitable for intermediate intervals, i.e. $9 < M(g) \leq 10$ and $10 < M(g) \leq 11$. Thus, we confirmed the work of Phleps et al. (2000) who showed that the observational based density functions for thin disc fit to two density laws, sech and exponential.

Comparison of the scaleheights and scalelengths of six fields, for the same absolute magnitude intervals, with their longitudes indicate that these parameters are longitude dependent. However, the correlation for the scalelength is not as high as for the scaleheight one. Additionally the errors for the scalelength are larger than the errors for the scaleheight. Alternatively, one may argue that tendency of the scaleheight and scalelength may due to the effect of the thick disc and/or halo stars at different distances from the Galactic center at different longitudes. However, as we mentioned above (Section 5.1) the contamination of the thick disc is rather small. Hence this argument is out of question in our work. It is worthwhile to remind that our sample stars in a field are at distances less than $r \sim 2$ kpc relative to the Sun, hence their distances from the Galactic center do not differ considerably from each other.

One may think that the argument stated in the former paragraph is in contradiction with the double exponential structure of the thin disc. Whereas we think in a different way. We do not reject the double exponential structure of the thin disc. However, we argue that additional constraints should be added for the refinement of scaleheight and scalelength of the thin disc (and the thick disc).

Finally, we compare scaleheights and scalelengths with the ones of Chen et al. (2001), Du et al. (2003) and Phleps et al. (2005). These authors give larger scaleheights than the mean scaleheight, $\langle H \rangle = 221$ pc, in our work for fields with larger Galactic longitudes, i.e. Chen et al. (2001): $310 < H < 345$ pc, $80^\circ < l < 180^\circ$ and $250^\circ < l < 360^\circ$; Du et al. (2003): $H = 320$ pc, $l = 169.95$; and Phleps et al. (2005): $H = 281/283$ pc, $85^\circ < l < 335^\circ$.

According to the relation between the scaleheight and the Galactic longitude given in this work we expect larger scaleheights for larger Galactic longitudes. Hence, the scaleheights presented in this work are in agreement with those appeared recently. The difference between our work and the others is that we argue and show the dependence of the scaleheight on the Galactic longitude.

The mean scalelength in our work, $h = 1900$ pc, is close to the ones adopted by Chen et al. (2001), $h = 2250$ pc, and Phleps et al. (2005), $h = 2000$ pc for estimation of the scaleheights in their work.

7 Acknowledgments

This work was supported by the Research Fund of the University of Istanbul. Project number: BYP 706/07062005.

A Appendix: Reduction of the secans hiperbolicus and secans hiperbolicus square scaleheights to the exponential one

The secans hiperbolicus is the sum of two exponentials, i.e.

$$\text{sech}(x) = 2/[\exp(-x) + \exp(x)]. \quad (\text{A.1})$$

Hence, the sech density law,

$$\text{sech}(-z/z_o) = 2/[\exp(-z/z_o) + \exp(z/z_o)]. \quad (\text{A.2})$$

Here z_o is the sech scaleheight. Now let us write the exponential density law, $\exp(-z/H)$, and equalize it to the sech density law:

$$\exp(-z/H) = 2/[\exp(-z/z_o) + \exp(z/z_o)], \quad (\text{A.3})$$

If we replace $z = H$, we find the equation $\exp(-1) = 2/[\exp(-H/z_o) + \exp(H/z_o)]$ which procudes $H/z_o = 1.65745$ or $H = 1.65745z_o$. This relation is in agreement with given by Phleps et al. (2000). For sech^2 , if we take the square of both sides in (A.2) and equalize it to the exponential density law:

$$\exp(-z/H) = 4/[\exp(-2z/z_o) + \exp(2z/z_o) + 2]. \quad (\text{A.4})$$

Also if we replace $z = H$, we find $\exp(-1) = 4/[\exp(-2H/z_o) + \exp(2H/z_o) + 2]$. The solution of this equation produces $H = 1.08504z_o$.

B Appendix: Reduction of the standard local space densities of Hipparcos to the *SDSS* photometry

The standard local space densities of Hipparcos (Jahreiss & Wielen, 1997) were reduced to the *SDSS* photometry, where the relation between $(B - V)$ and $M(V)$ derived for the main-sequence stars within 10 pc of the Sun by Henry et al. (1999), were used in order to transform $M(V)$ absolute magnitudes of the Yale Parallax Catalog (van Altena et al., 1998) and the Hipparcos mission (ESA, 1997) to the $(B - V)$ colour indices, i.e.

$$(B - V) = 0.00099M(V)^3 - 0.038184M(V)^2 + 0.555204M(V) - 1.242359. \quad (\text{B.1})$$

Then, we used the equation of Bilir, Karaali & Tunçel (2005) to derive the $M(g)$ absolute magnitudes of *SDSS* photometry:

$$M(g) = M(V) + 0.63359(B - V) - 0.10813. \quad (\text{B.2})$$

Finally, the standard local space densities of Hipparcos (Jahreiss & Wielen, 1997) for the absolute magnitudes of $M(g)$: 7.5, 8.5, 9.5, 10.5 and 11.5, were interpolated and is given in the column (13) of Table 4.

References

- Bahcall, J.N., Soneira, R.M., 1980, ApJ, 238L, 17
 Bilir, S., Karaali, S., Tunçel, S., 2005, AN, 326, 321
 Bilir, S., Karaali, S., Gilmore, G., 2006, MNRAS, 366, 1295 (BKG)
 Buser, R., Rong, J., Karaali, S., 1998, A&A, 331, 934
 Buser, R., Rong, J., Karaali, S., 1999, A&A, 348, 98
 Chen, B., et al. (the SDSS Collaboration), 2001, ApJ, 553, 184
 de Grijs, R., Peletier, R.F., van der Kruit, P.C., 1997, A&A, 327, 966
 del Rio G., Fenkart, R.P., 1987, A&AS, 68, 397
 Du, C., Zhou, X., Ma, J., Bing-Chih, A., Yang, Y., Li, J., Wu, H., Jiang, Z.,
 Chen, J., 2003, A&A, 407, 541
 ESA, 1997, The Hipparcos and Tycho Catalogues, (ESA SP-1200) (Noordwijk: ESA)
 Fan, X., 1999, AJ, 117, 2528
 Fenkart, R.P., Topaktaş, L., Boydağ, S., Kandemir, G., 1987, A&AS, 67, 245

Gilmore, G., Reid, N., 1983, MNRAS, 202, 1025
Gilmore, G., 1984, MNRAS, 207, 223
Henry, T.J., Franz, O.G., Wasserman, L.H., Benedict, G.F., Shelus, P.J., Ianna, P.A., Kirkpatrick, J.D., McCarthy, D.W., 1999, ApJ, 512, 864
Jahreiss, H., Wielen, R., 1997, in Battrick, B., Perryman, M.A.C., & Bernacca, P.L., eds, HIPPARCOS - Venice '97. ESA SP-402, Noordwijk, p. 675
Jurić, M., et al., 2005, astro-ph/0510520
Karaali, S., Bilir, S., Hamzaoglu, E., 2004, MNRAS, 355, 307 (KBH)
Kuijken, K., Gilmore, G., 1989, MNRAS, 239, 605
Larsen, J.A., 1996, Ph. D. Thesis, Univ. Minnesota
O'Connell, D.J.K., ed. 1958. Stellar Populations. Amsterdam: North Holland Press. Oort, J.H., 1958. In O'Connell, p.419
Ojha, D.K., Bienaymé, O., Mohan, V., Robin, A.C., 1999, A&A, 351, 945
Phleps, S., Meisenheimer, K., Fuchs, B., Wolf, C., 2000, A&A, 356, 108
Phleps, S., Drepper, S., Meisenheimer, K., Fuchs, B., 2005, A&A, 443, 929
Reid, N., Majewski, S.R., 1993, ApJ, 409, 635
Robin, A.C., Crézé, M., 1986, A&A, 157, 71
Robin, A.C., Haywood, M., Crézé, M., Ojha, D.K., Bienaymé, O., 1996, A&A, 305, 125
Robin, A.C., Reylé, C., Crézé, M., 2000, A&A, 359, 103
Schlegel, D.J., Finkbeiner, D.P., Davis, M., 1998, ApJ, 500, 525
Siegel, M.H., Majewski, S.R., Reid, I.N., Thompson, I.B., 2002, ApJ, 578, 151
Tritton, K.P., Morton, D.C., 1984, MNRAS, 209, 429
van Altena, W.F., Lee, J.T., & Hoffleit, E.D., 1995, The General Catalogue of Trigonometric Stellar Parallaxes (4th ed.; New Haven: Yale Univ. Obs.)
von Hippel, T., Bothun, G.D., 1993, ApJ, 407, 115
Yamagata, T., Yoshii, Y., 1992, AJ, 103, 117
Yoshii, Y., 1982, PASJ, 34, 365
Yoshii, Y., Ishida, K., Stobie, R.S., 1987, AJ, 93, 323

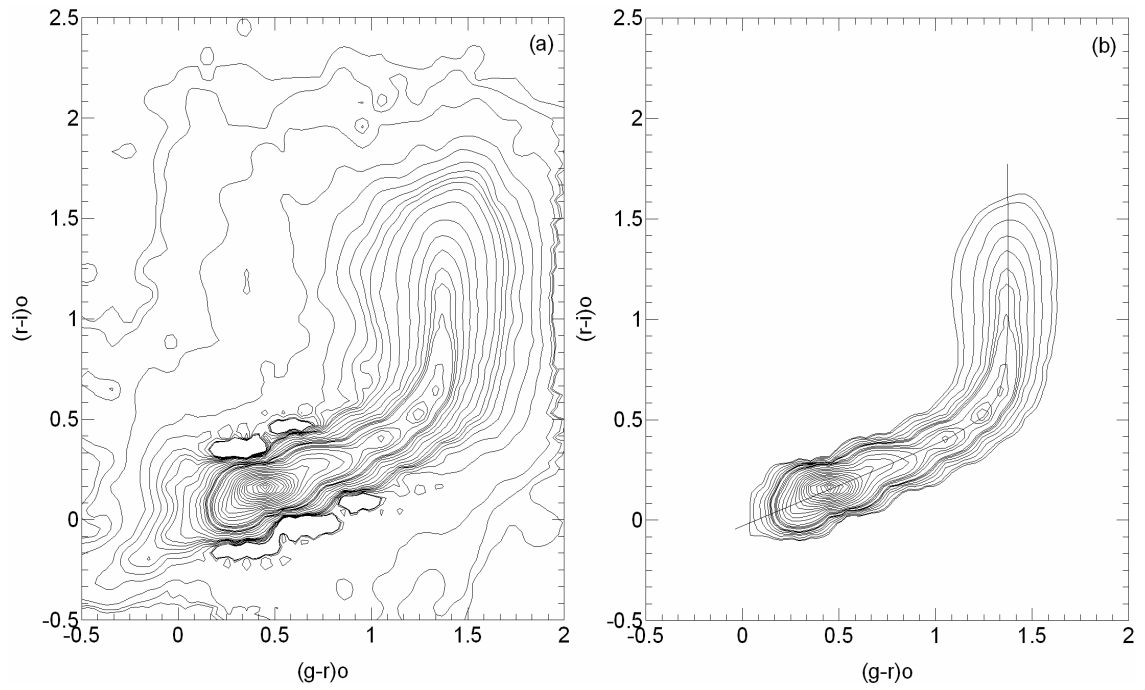


Fig. 1. Isodensity contours for the objects after performing the star/galaxy separation by using the *SDSS* photometric pipeline (a). Objects at distances larger than 0.3 mag from the locus were rejected from the sample (b). The procedure is adopted from Jurić et al. (2005).

Table 1

Previous Galactic models. Symbols: H: scaleheight, h: scalelength, n: local space density of the population relative to the space density of the thin disc, R_e : the effective radius, and $\kappa = c/a$: the axis ratio.

Thin disc			Thick disc			Halo		Reference
H (pc)	h (kpc)	n_{thick}	H (kpc)	h (kpc)	n_{halo}	R_e (kpc)	κ	
310-325	—	0.0125-0.025	1.92-2.39	—	—	—	—	Yoshii (1982)
300	—	0.02	1.45	—	0.0020	3.0	0.85	Gilmore & Reid (1983)
325	—	0.02	1.3	—	0.0020	3.0	0.85	Gilmore (1984)
280	—	0.0028	1.9	—	0.0012	—	—	Tritton & Morton (1984)
200-475	—	0.016	1.18-2.21	—	0.0016	—	0.80	Robin & Crézé (1986)
300	—	0.02	1.0	—	0.0010	—	0.85	del Rio & Fenkart (1987)
285	—	0.015	1.3-1.5	—	0.0020	2.36	flat	Fenkart et al. (1987)
325	—	0.0224	0.95	—	0.0010	2.9	0.90	Yoshii et al. (1987)
249	—	0.041	1.0	—	0.0020	3.0	0.85	Kuijken & Gilmore (1989)
350	3.8	0.019	0.9	3.8	0.0011	2.7	0.84	Yamagata & Yoshii (1992)
290	—	—	0.86	—	—	4.0	—	von Hippel & Bothun (1993)
325	—	0.0225	1.5	—	0.0015	3.5	0.80	Reid & Majewski (1993)
325	3.2	0.019	0.98	4.3	0.0024	3.3	0.48	Larsen (1996)
250-270	2.5	0.056	0.76	2.8	0.0015	2.44-2.75 ^a	0.60-0.85	Robin et al. (1996, 2000)
290	4.0	0.059	0.91	3.0	0.0005	2.69	0.84	Buser, Rong & Karaali (1998, 1999)
240	2.5	0.061	0.79	2.8	—	—	0.60-0.85	Ojha et al. (1999)
330	2.25	0.065-0.13	0.58-0.75	3.5	0.0013	—	0.55	Chen et al. (2001)
280	2-2.5	0.06-0.10	0.7-1.0	3-4	0.0015	—	0.50-0.70	Siegel et al. (2002)
350	2-2.5	0.06-0.10	0.9-1.2	3-4	0.0015	—	0.50-0.70	Siegel et al. (2002) ^b
320	—	0.07	0.64	—	0.0013	—	0.58	Du et al. (2003)

a Power-law index replacing R_e .

b Corrected values for binarism.

Table 2

Data for six fields investigated in this work. The coordinates are for the epoch 2000, and **N** is the number of stars.

Field	α	δ	l	b	Size	$E(B - V)$	N
	(h m s)	($^{\circ}$ ' ")	($^{\circ}$)	($^{\circ}$)	(deg ²)		
F1	15 34 14	-00 22 44	4.58	42.19	10	0.102	20 549
F2	15 40 00	08 30 00	15.93	46.06	10	0.044	19 198
F3	16 30 00	24 06 00	42.28	41.02	10	0.059	25 577
F4	16 02 22	38 38 19	61.62	48.78	10	0.013	14 523
F5	15 42 00	44 24 00	71.29	51.89	10	0.019	8 731
F6	09 52 00	52 45 00	83.38	48.55	20	0.015	24 802

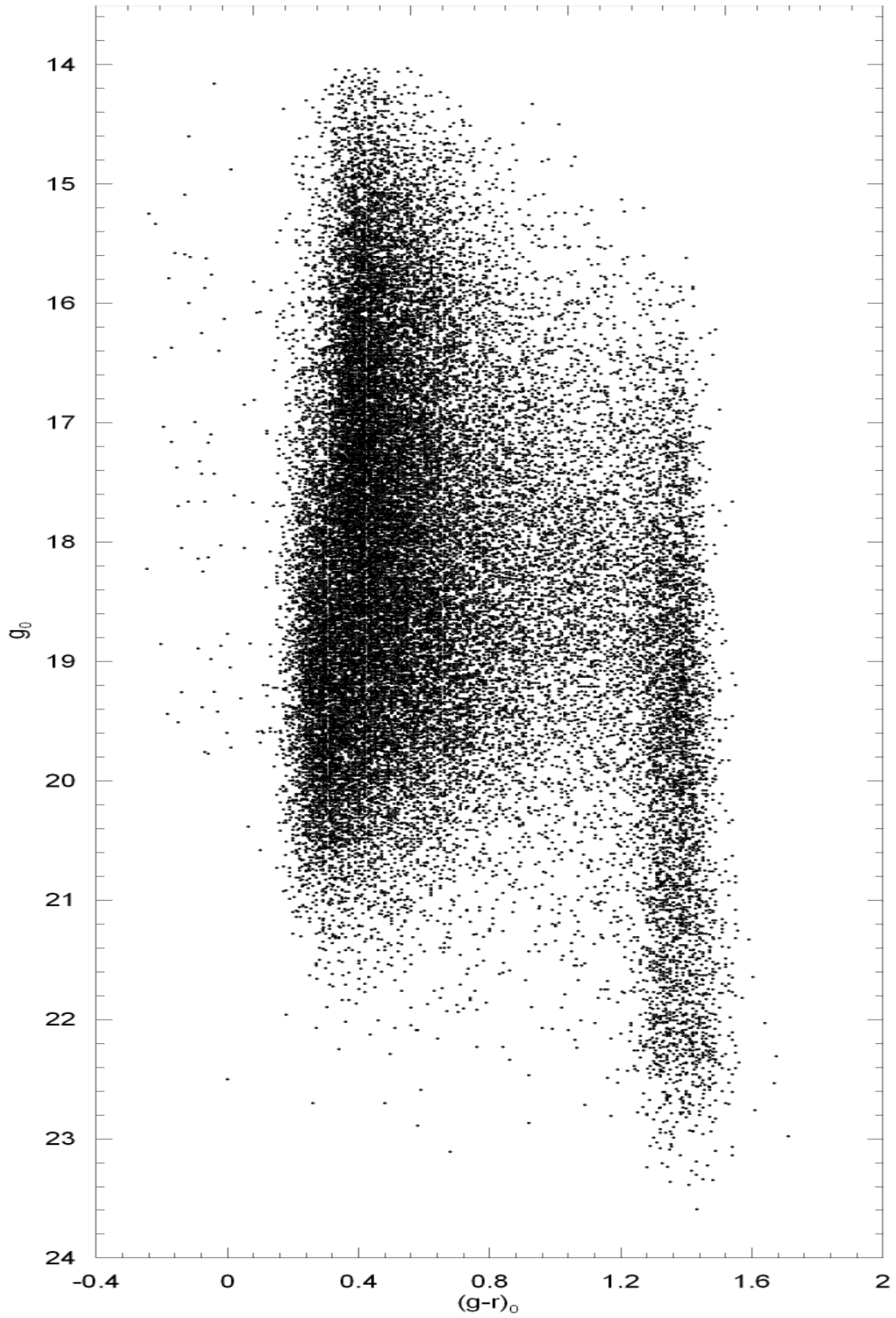


Fig. 2. Apparent magnitude colour diagram for the star sample in consideration.

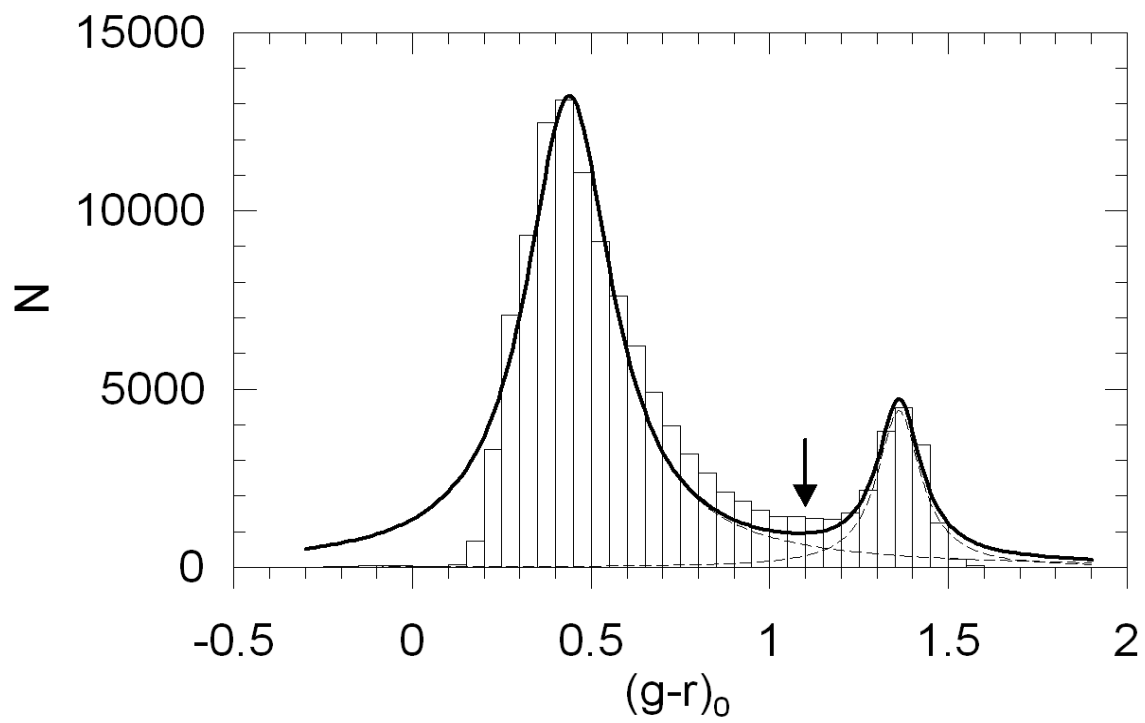


Fig. 3. $(g-r)_o$ histogram for the star sample used to separate the thin-disc stars.

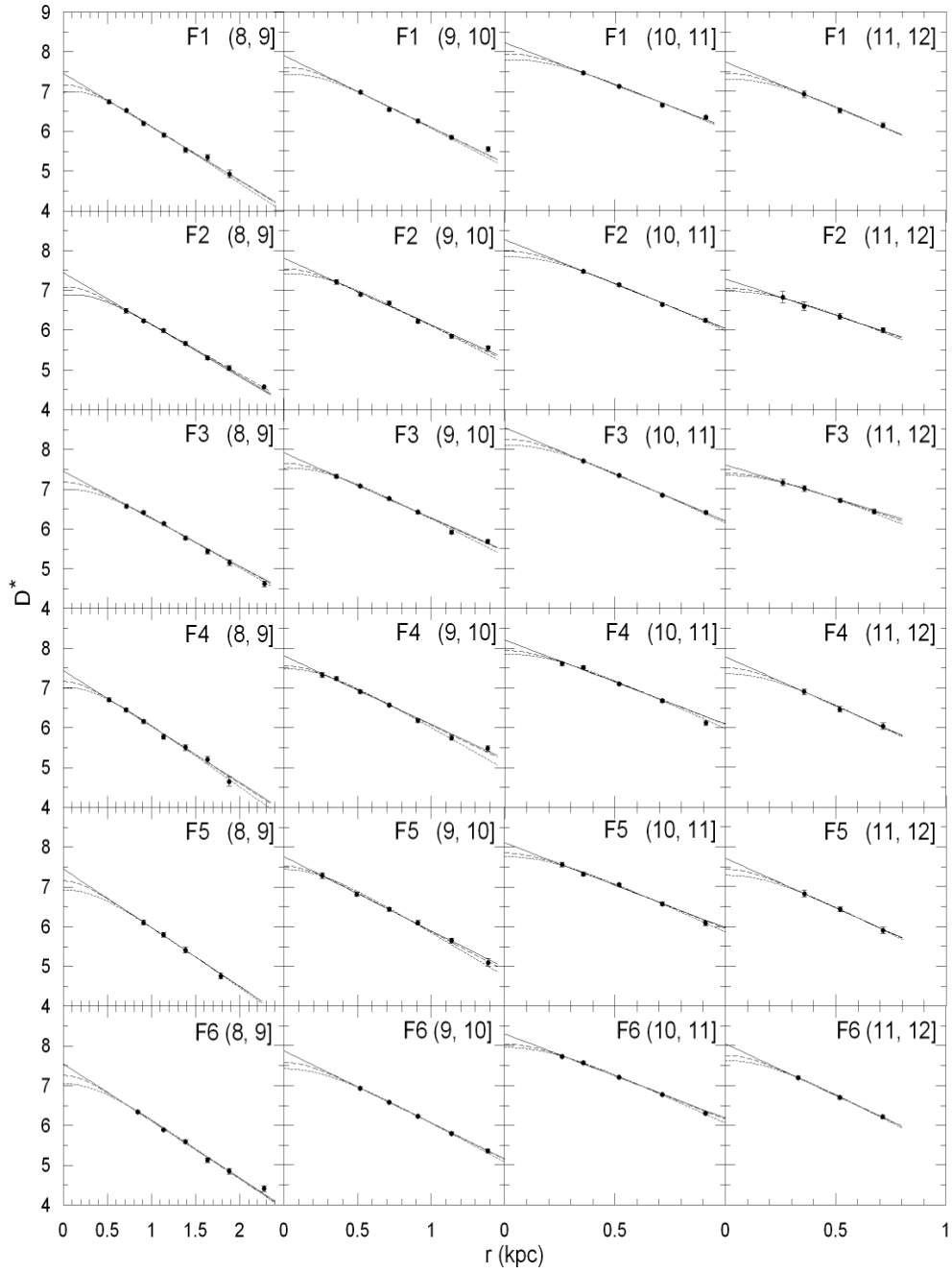


Fig. 4. Comparison of derived thin disc space density functions (symbols) with the best fit analytical density laws (lines) for different absolute magnitude intervals for six fields. The continuous curve represents the exponential law, the dashed curve represent the sech law and the dot-dashed curve represents the sech^2 law in the vertical direction.

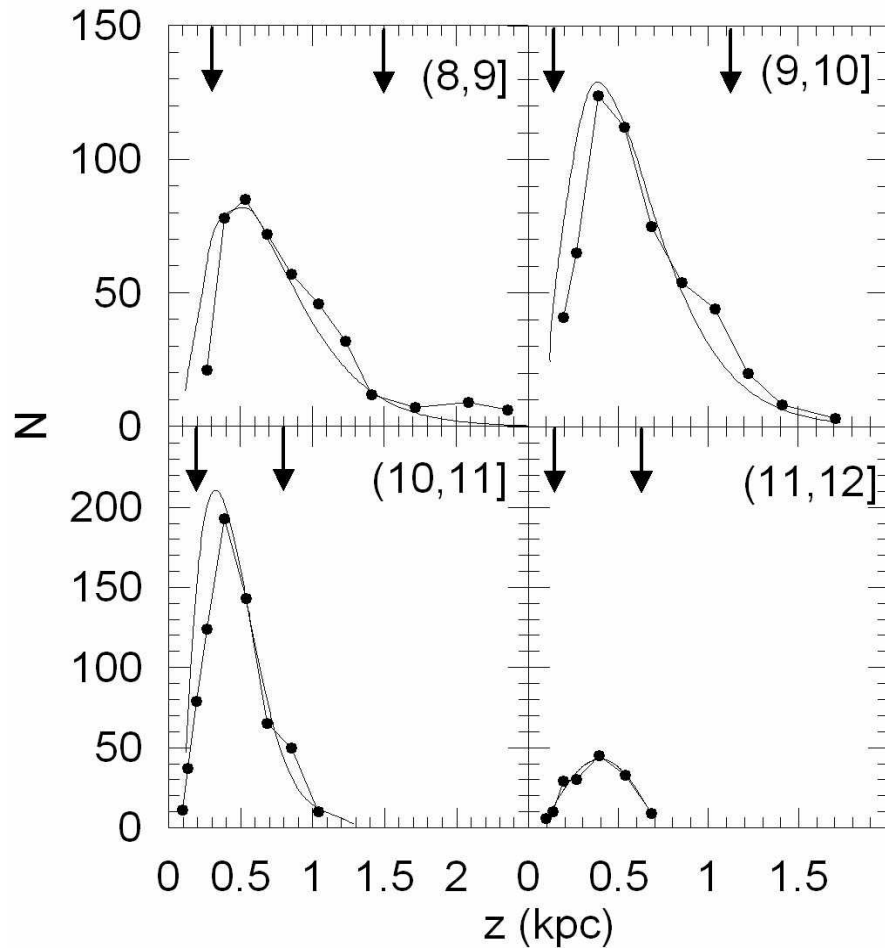


Fig. 5. Fitting of the distribution of z -distances for stars in four absolute magnitude intervals for the Field F4 with a curve of single mode indicating the thin disc. There are slight differences between the number of observed stars and the predicted ones. The arrows at the top each panel show the limiting completeness of z -distances for the bright and faint apparent magnitudes.

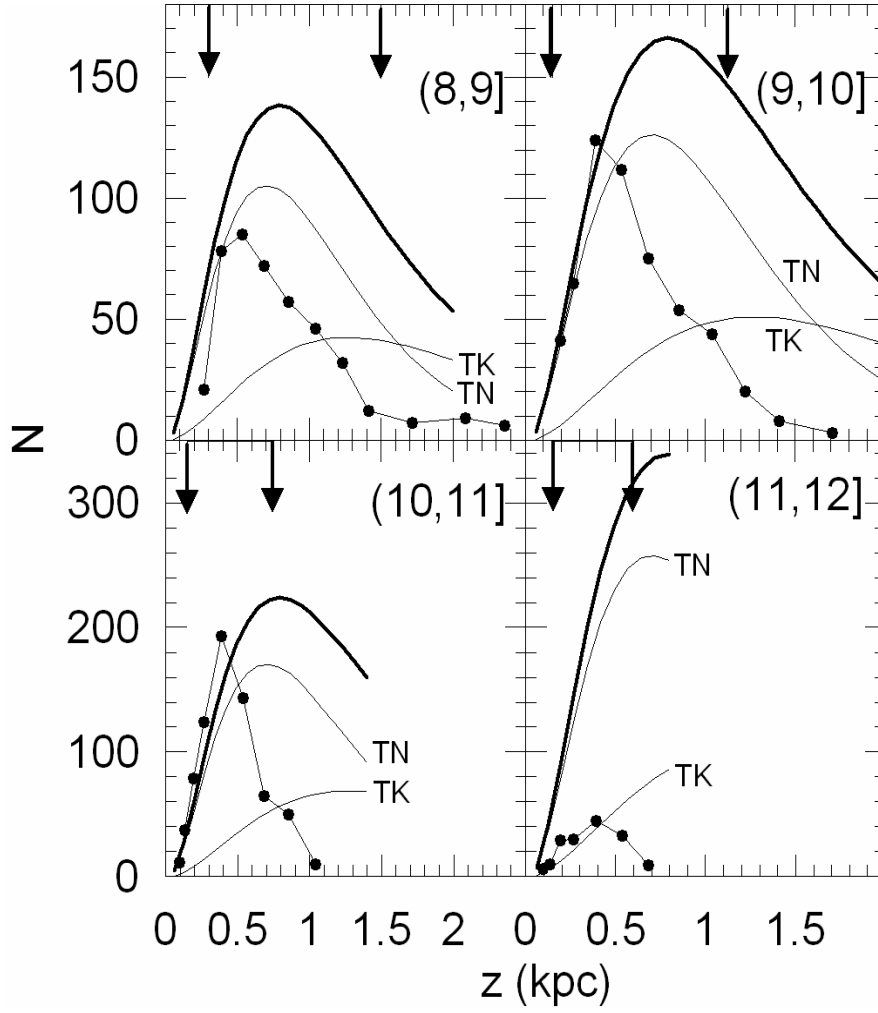


Fig. 6. Comparison of the distribution of distances above the Galactic plane for stars in the field F4, as an example, with the Galactic model of Chen et al. (2001). The scaleheight and solar normalization of the thick disc are $H = 600$ pc, $n_2/n_1 = 12$ per cent, respectively. Small differences between the number of stars and the predicted ones for the thin disc (TN) indicate slight contamination of thick disc (TK). Arrows are as in the Fig. 5.

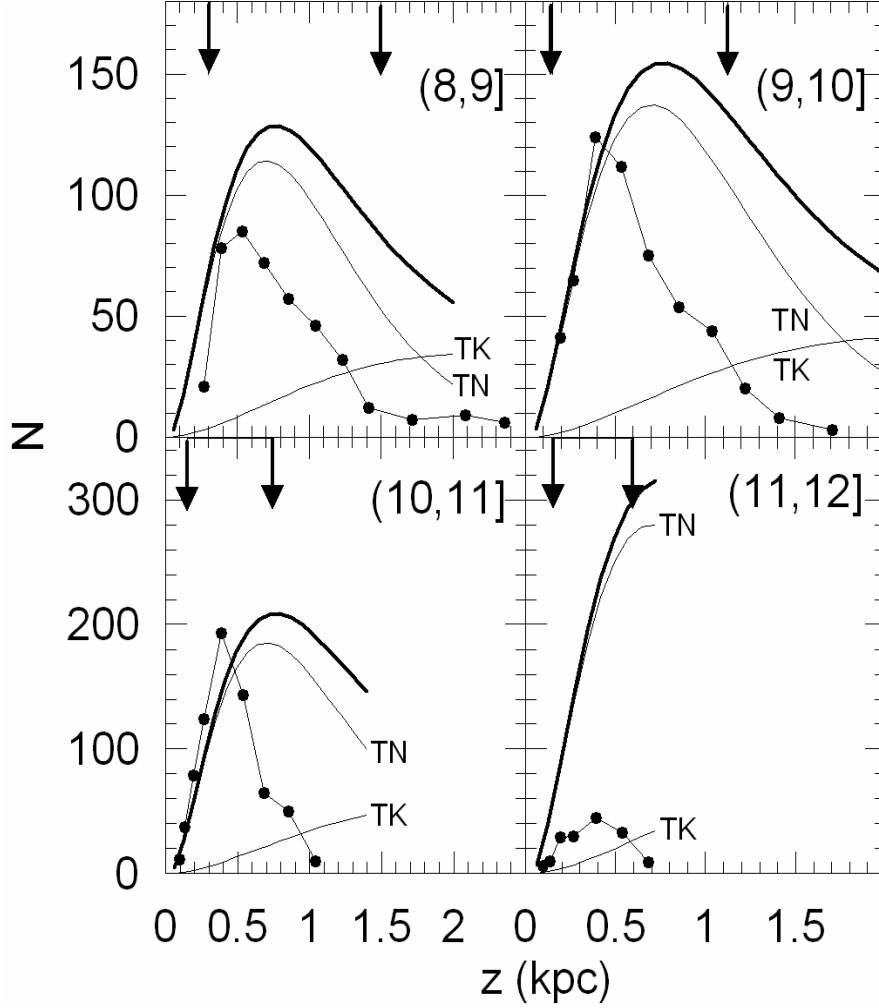


Fig. 7. Comparison of the distribution of distances above the Galactic plane for stars in the field F4, as an example, with the Galactic model of Chen et al. (2001). The scaleheight and solar normalization of the thick disc are $H = 1000$ pc, $n_2/n_1 = 3$ per cent, respectively. The other model parameters are the same as in Fig. 6. The same small discrepancy in Fig. 6 can be seen also here. Arrows are as in the Fig. 5.

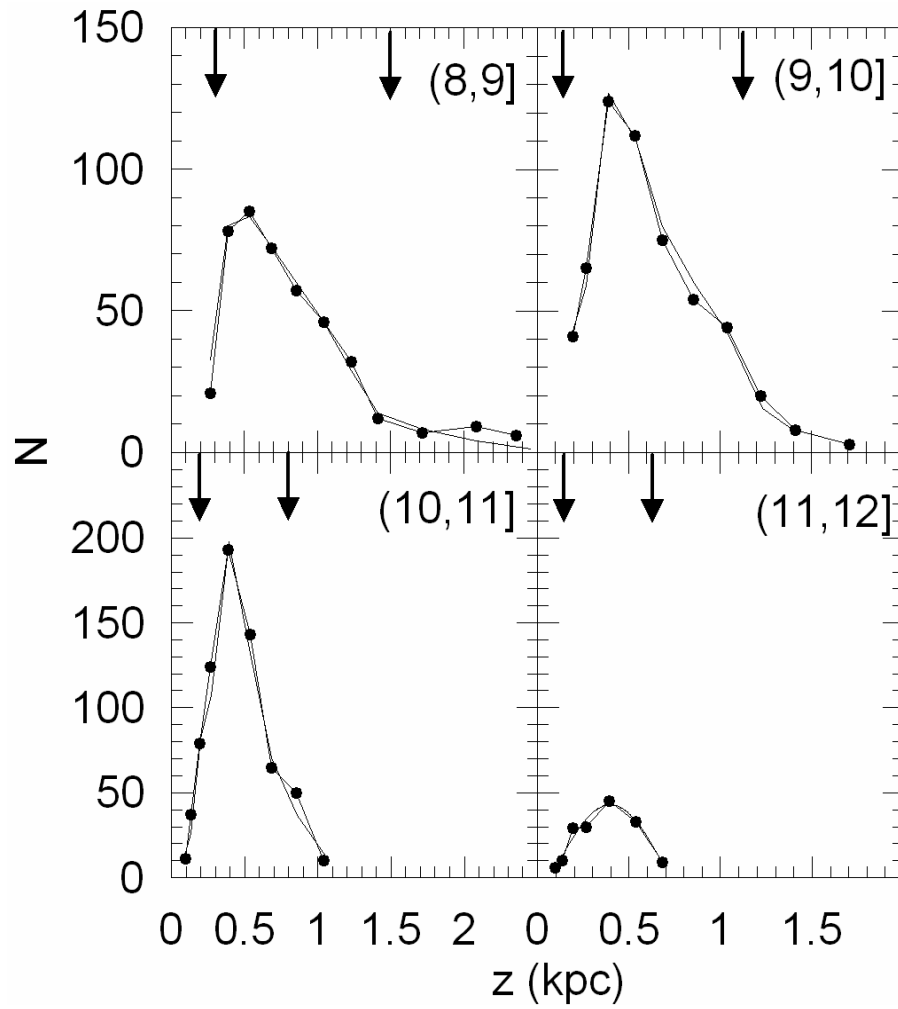


Fig. 8. Reduction of the number of stars by 7, 14, 16 per cent for the absolute magnitude intervals $8 < M(g) \leq 9$, $9 < M(g) \leq 10$, and $10 < M(g) \leq 11$ brings the observed number of stars close to the predicted ones. Arrows are as in the Fig. 5.

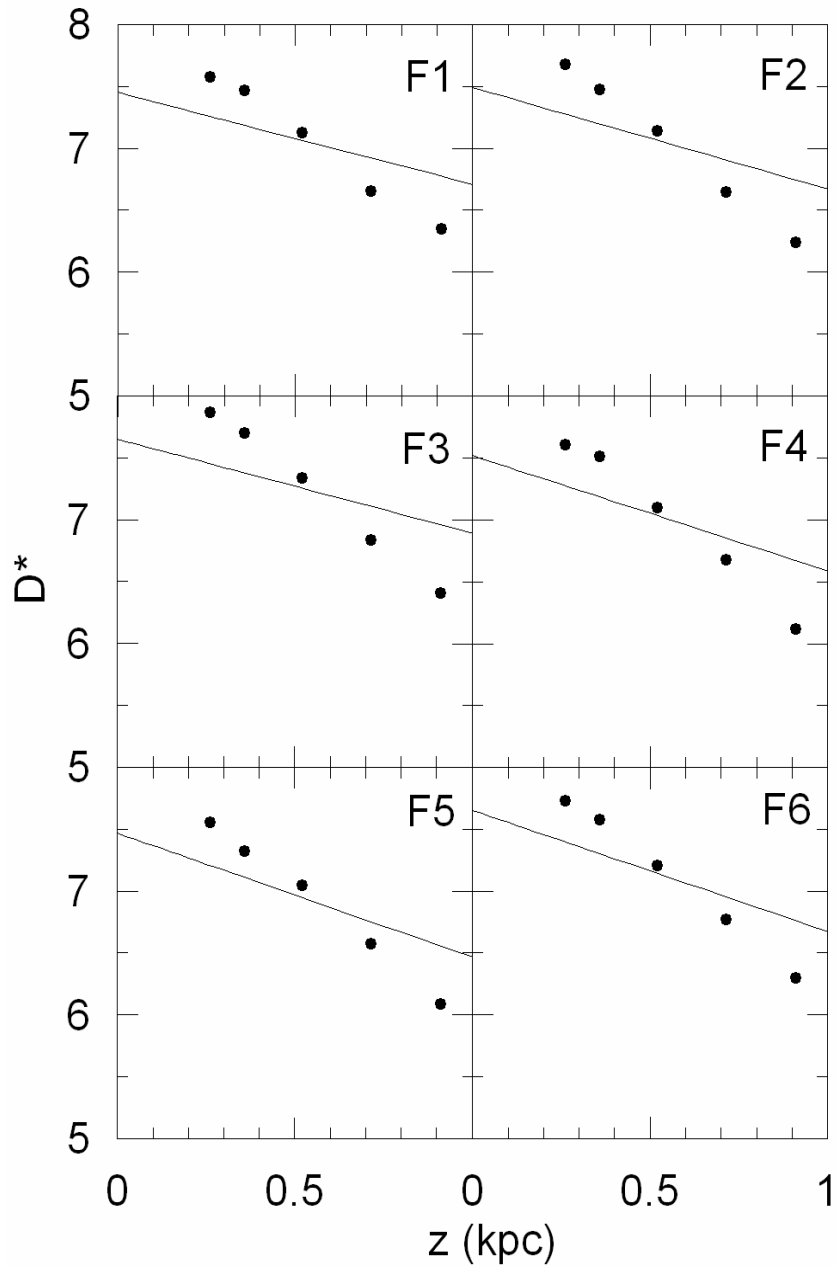


Fig. 9. Comparison of the derived logarithmic space densities D^* with the Galactic disc model of Chen et al. (2001) for stars with absolute magnitudes $10 < M(g) \leq 11$, for six fields. Agreement is rather poor and the standard deviations are large (see Table 5).

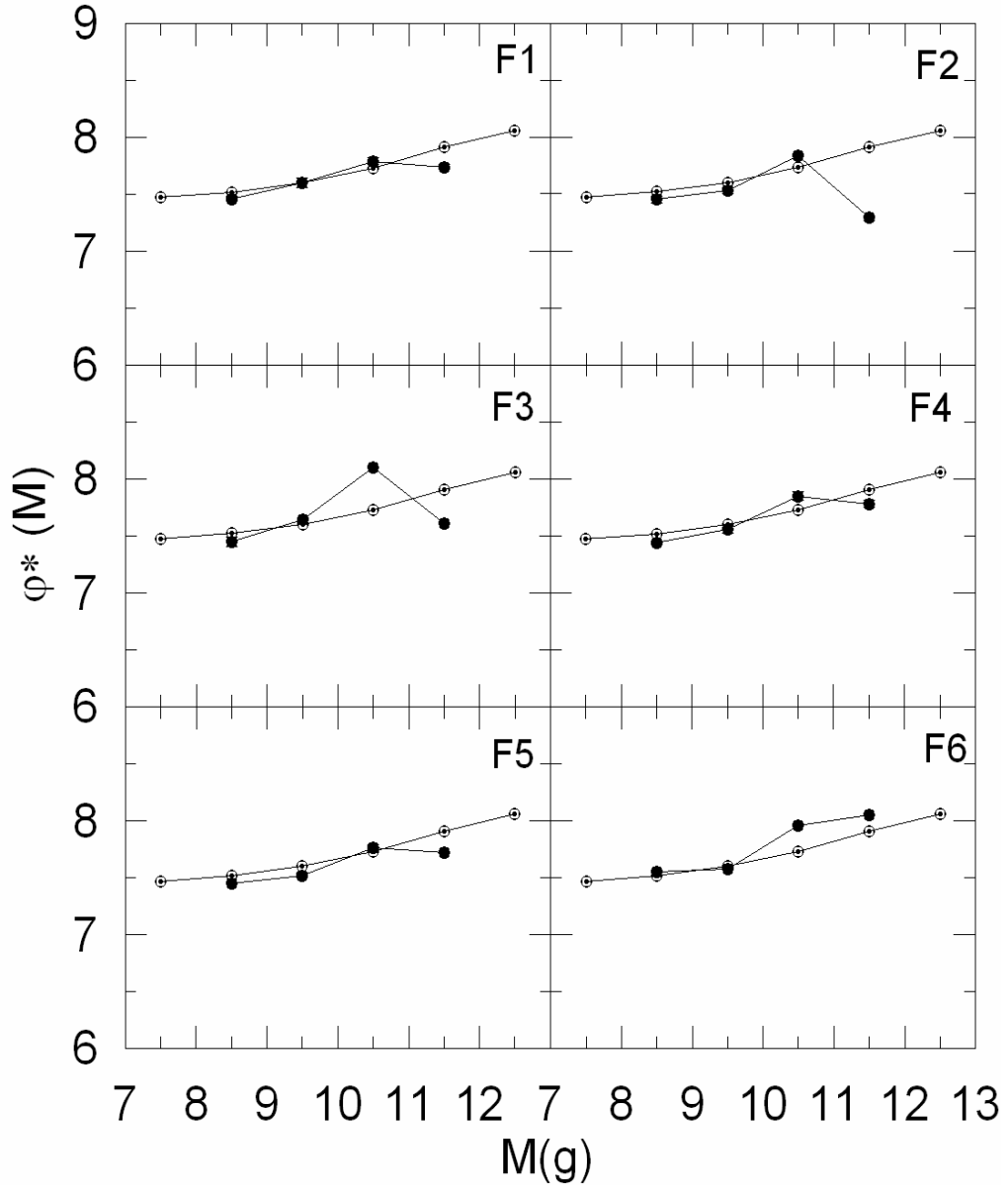


Fig. 10. The local luminosity function for the thin disc. The \odot symbols indicate the Hipparcos standard values.

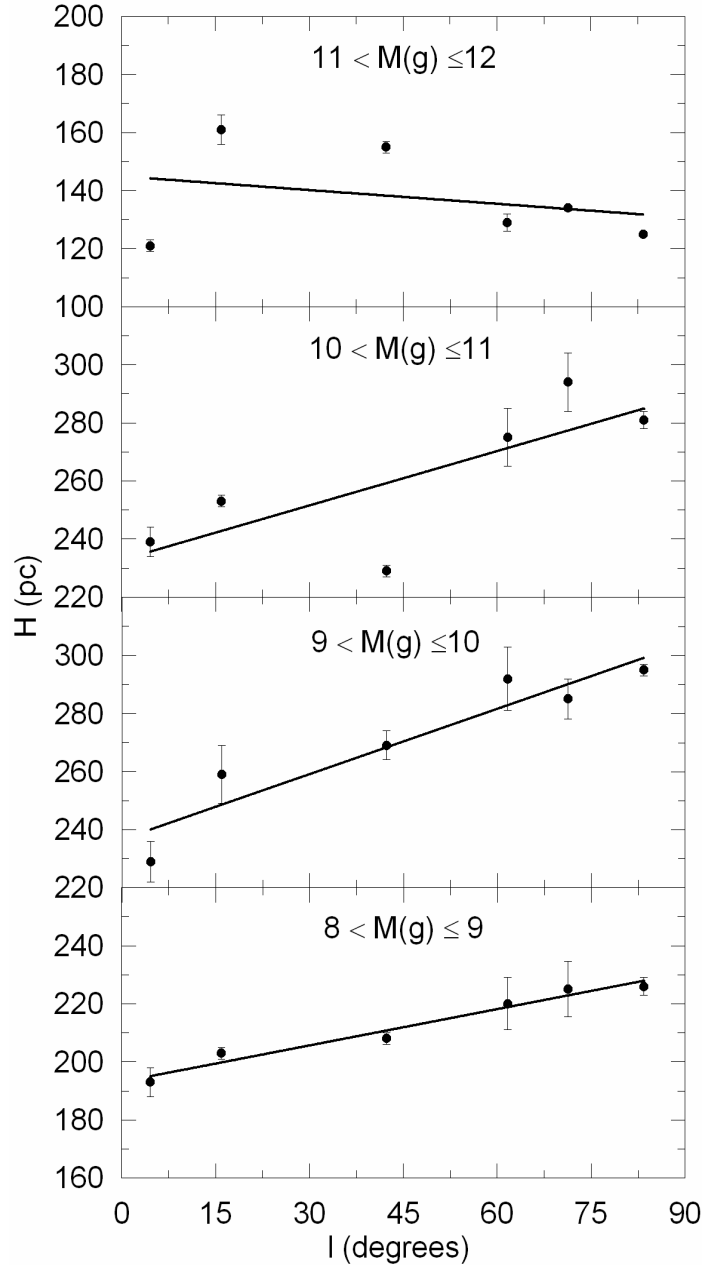


Fig. 11. The relation between the scaleheights for six fields and the corresponding Galactic longitudes.

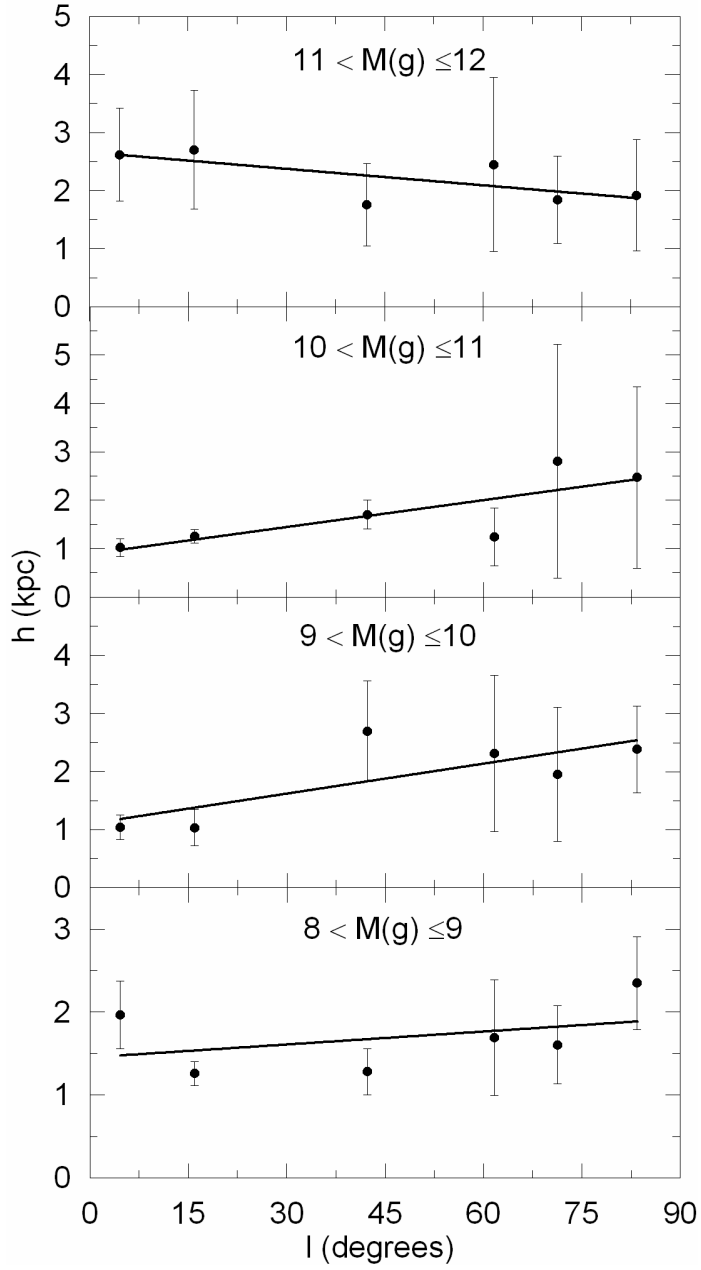


Fig. 12. The relation between the scalelengths for six fields and the corresponding Galactic longitudes.

Table 3

Logarithmic space density function, $D^* = \log D + 10$, for different absolute magnitude intervals for the Field F4 as an example. Distances in kpc, volumes in pc^3 , horizontal lines show the limiting distance of completeness. Other symbols are explained in the text.

$M(g) \rightarrow$			(8,9]		(9,10]		(10,11]		(11,12]		(12,13]	
$r_1 - r_2$	$\Delta V_{1,2}$	r^*	N	D^*	N	D^*	N	D^*	N	D^*	N	D^*
0.10-0.15	2.41 (3)	0.13					11	7.66	6	7.40		
0.15-0.20	4.70 (3)	0.18					37	7.90	10	7.33		
0.20-0.30	1.93 (4)	0.26			41	7.33	79	7.61	29	7.18	1	5.71
0.30-0.40	3.76 (4)	0.36	21	6.75	65	7.24	124	7.52	30	6.90		
0.40-0.60	1.54 (5)	0.52	78	6.70	124	6.90	193	7.10	45	6.46		
0.60-0.80	3.01 (5)	0.71	85	6.45	112	6.57	143	6.68	33	6.04		
0.80-1.00	4.96 (5)	0.91	72	6.16	75	6.18	65	6.12	9	5.26		
1.00-1.25	9.68 (5)	1.14	57	5.77	54	5.75	50	5.71				
1.25-1.50	1.44 (6)	1.39	46	5.50	44	5.48	10	4.84				
1.50-1.75	2.01 (6)	1.64	32	5.20	20	5.00						
1.75-2.00	2.68 (6)	1.88	12	4.65	8	4.47						
2.00-2.50	7.74 (6)	2.28	7	3.96	3	3.59						
2.50-3.00	1.16 (7)	2.77	9	3.89								
3.00-3.50	1.61 (7)	3.27	6	3.57								
Total			425		546		712		162		1	

Table 4

Galactic model parameters for different absolute magnitude intervals for the thin disc of six fields, resulting from the fits of derived and analytical density profiles. The columns indicate: (1) absolute magnitude interval $M(g)$, (2) density law, (3) and (8) logarithmic local space density n^* , (4) and (9) standard deviation for logarithmic space density s , (5) and (10) scaleheight (in pc) reduced to the exponential law H , (6) and (11) scalelength (in pc) h , (7) and (12) χ^2_{min} , and (13) the standard local space density of Hipparcos reduced to the *SDSS* photometry \odot (see Appendix B).

(1)	(2)	(3)	(4)	(5)	(6)	(7)	(8)	(9)	(10)	(11)	(12)	(13)
M(g)	law	n^*	s	H	h	χ^2_{min}	n^*	s	H	h	χ^2_{min}	\odot
Field 1												
(8,9]	exp	7.46 ^{+0.02} _{-0.02}	0.05	193 ⁺⁴ ₋₄	1967 ⁺⁴⁹⁰ ₋₃₃₀	3.73	7.44 ^{+0.02} _{-0.02}	0.06	220 ⁺⁴ ₋₄	1690 ⁺⁹⁴⁰ ₋₄₅₀	3.34	7.52
	sech	7.17 ^{+0.02} _{-0.02}	0.05	322 ⁺⁷ ₋₇	2169 ⁺⁵⁸⁰ ₋₃₈₀	3.82	7.16 ^{+0.02} _{-0.02}	0.06	360 ⁺⁷ ₋₇	1675 ⁺⁹⁷⁰ ₋₄₅₀	3.35	
	sech ²	6.98 ^{+0.03} _{-0.03}	0.06	333 ⁺⁷ ₋₇	704 ⁺⁶² ₋₅₀	6.26	7.01 ^{+0.03} _{-0.03}	0.06	427 ⁺⁹ ₋₁₀	1158 ⁺⁶²⁰ ₋₂₄₀	3.80	
(9,10]	exp	7.90 ^{+0.04} _{-0.04}	0.08	150 ⁺⁵ ₋₅	2300 ⁺¹⁷⁵⁰ ₋₇₀₀	8.99	7.81 ^{+0.04} _{-0.04}	0.06	183 ⁺⁹ ₋₈	2546 ⁺¹⁸⁸⁰ ₋₁₅₆₀	6.05	7.60
	sech	7.60 ^{+0.04} _{-0.04}	0.08	229 ⁺⁷ ₋₇	1038 ⁺²⁵⁵ ₋₁₇₀	8.98	7.56 ^{+0.03} _{-0.03}	0.06	292 ⁺¹² ₋₁₀	2313 ⁺¹⁴⁵⁰ ₋₁₂₅₀	5.65	
	sech ²	7.42 ^{+0.06} _{-0.04}	0.10	277 ⁺¹² ₋₈	935 ⁺²⁰⁰ ₋₁₉₅	14.74	7.48 ^{+0.02} _{-0.02}	0.06	321 ⁺⁹ ₋₉	1030 ⁺⁷⁵⁰ ₋₃₀₀	5.80	
(10,11]	exp	8.23 ^{+0.02} _{-0.02}	0.06	129 ⁺² ₋₁	2417 ⁺¹¹²⁰ ₋₅₈₀	7.13	8.21 ^{+0.06} _{-0.06}	0.08	148 ⁺¹¹ ₋₉	1589 ⁺¹²⁰⁰ ₋₁₀₁₀	12.43	7.73
	sech	7.94 ^{+0.02} _{-0.02}	0.05	197 ⁺³ ₋₂	1039 ⁺¹⁶⁵ ₋₁₃₀	4.21	7.94 ^{+0.05} _{-0.04}	0.08	242 ⁺¹⁵ ₋₁₃	1867 ⁺¹⁴¹⁰ ₋₁₁₇₅	11.11	
	sech ²	7.79 ^{+0.03} _{-0.03}	0.04	239 ⁺⁵ ₋₅	1022 ⁺²²⁰ ₋₁₅₀	4.04	7.85 ^{+0.04} _{-0.04}	0.04	275 ⁺¹⁰ ₋₁₀	1237 ⁺⁶⁵⁰ ₋₅₄₅	4.70	
(11,12]	exp	7.74 ^{+0.02} _{-0.02}	0.03	121 ⁺² ₋₂	2619 ⁺¹⁰⁵⁰ ₋₅₄₀	0.66	7.78 ^{+0.03} _{-0.03}	0.03	129 ⁺³ ₋₃	2448 ⁺¹⁶⁰⁰ ₋₁₄₀₀	0.37	7.91
	sech	7.45 ^{+0.02} _{-0.02}	0.03	192 ⁺³ ₋₃	1516 ⁺⁴⁴⁰ ₋₂₈₀	0.68	7.50 ^{+0.03} _{-0.03}	0.03	209 ⁺⁵ ₋₅	1730 ⁺⁷⁴⁰ ₋₆₀₀	0.45	
	sech ²	7.30 ^{+0.03} _{-0.03}	0.04	232 ⁺⁷ ₋₅	1454 ⁺⁵⁸⁰ ₋₃₂₅	1.19	7.35 ^{+0.03} _{-0.03}	0.04	252 ⁺⁵ ₋₅	1580 ⁺⁸⁸⁰ ₋₆₃₀	0.80	
Field 2												
(8,9]	exp	7.45 ^{+0.02} _{-0.03}	0.03	203 ⁺³ ₋₃	1260 ⁺¹⁷⁰ ₋₁₂₀	0.84	7.45 ^{+0.01} _{-0.01}	0.03	225 ⁺² ₋₂	1606 ⁺⁶⁰⁰ ₋₃₄₅	0.59	7.52
	sech	7.08 ^{+0.01} _{-0.01}	0.04	255 ⁺³ ₋₃	1326 ⁺⁸⁰ ₋₇₅	3.73	7.15 ^{+0.01} _{-0.01}	0.03	373 ⁺³ ₋₃	1625 ⁺⁶⁴⁵ ₋₃₆₀	0.59	
	sech ²	6.87 ^{+0.01} _{-0.01}	0.04	408 ⁺³ ₋₃	808 ⁺³⁴ ₋₃₂	1.68	6.92 ^{+0.01} _{-0.01}	0.03	465 ⁺³ ₋₃	1030 ⁺¹⁵⁵ ₋₁₂₅	0.65	
(9,10]	exp	7.81 ^{+0.04} _{-0.04}	0.06	162 ⁺⁶ ₋₆	1135 ⁺⁴⁵⁰ ₋₂₅₀	10.31	7.76 ^{+0.01} _{-0.01}	0.04	180 ⁺³ ₋₃	2080 ⁺¹¹⁸⁰ ₋₉₈₀	2.50	7.60
	sech	7.53 ^{+0.05} _{-0.03}	0.06	259 ⁺¹³ ₋₇	1030 ⁺³⁵⁰ ₋₂₇₅	10.06	7.52 ^{+0.02} _{-0.02}	0.04	285 ⁺⁷ ₋₇	1950 ⁺¹²⁶⁰ ₋₁₀₅₀	1.54	
	sech ²	7.41 ^{+0.05} _{-0.05}	0.08	312 ⁺¹⁴ ₋₁₃	1051 ⁺⁴⁵⁵ ₋₂₄₅	13.65	7.44 ^{+0.05} _{-0.05}	0.07	333 ⁺¹⁴ ₋₁₇	2100 ⁺¹⁷¹⁰ ₋₁₄₂₅	8.70	
(10,11]	exp	8.28 ^{+0.02} _{-0.02}	0.02	124 ⁺² ₋₂	1024 ⁺⁵³⁰ ₋₅₀₀	1.30	8.11 ^{+0.02} _{-0.02}	0.04	155 ⁺⁸ ₋₈	1114 ⁺⁶⁴⁰ ₋₅₃₀	4.37	7.73
	sech	7.99 ^{+0.02} _{-0.02}	0.02	217 ⁺³ ₋₃	2150 ⁺⁶³⁰ ₋₄₀₀	1.47	7.85 ^{+0.03} _{-0.03}	0.04	254 ⁺⁵ ₋₅	2212 ⁺¹⁷²⁰ ₋₁₄₃₀	3.34	
	sech ²	7.84 ^{+0.01} _{-0.01}	0.02	253 ⁺² ₋₂	1250 ⁺¹⁶⁵ ₋₁₂₀	1.24	7.76 ^{+0.03} _{-0.03}	0.03	294 ⁺¹¹ ₋₁₀	2804 ⁺²⁴⁵⁰ ₋₂₀₃₀	1.68	
(11,12]	exp	7.29 ^{+0.02} _{-0.02}	0.02	161 ⁺⁵ ₋₅	2703 ⁺¹¹²⁰ ₋₉₃₀	0.17	7.72 ^{+0.01} _{-0.01}	0.02	134 ⁺¹ ₋₁	1845 ⁺⁸²⁵ ₋₆₈₅	0.15	7.91
	sech	7.04 ^{+0.03} _{-0.03}	0.03	234 ⁺⁸ ₋₇	1010 ⁺³¹⁰ ₋₂₁₀	0.38	7.44 ^{+0.01} _{-0.01}	0.02	219 ⁺² ₋₂	1826 ⁺⁷⁵⁰ ₋₆₂₅	0.17	
	sech ²	6.97 ^{+0.04} _{-0.04}	0.05	281 ⁺¹⁴ ₋₁₃	1841 ⁺⁹⁴⁰ ₋₇₀₀	0.78	7.29 ^{+0.01} _{-0.01}	0.02	264 ⁺¹ ₋₁	1604 ⁺³²⁰ ₋₂₂₀	0.18	
Field 3												
(8,9]	exp	7.45 ^{+0.04} _{-0.04}	0.05	208 ⁺⁶ ₋₆	1281 ⁺³⁴⁰ ₋₂₂₀	3.11	7.55 ^{+0.02} _{-0.02}	0.07	226 ⁺⁴ ₋₃	2350 ⁺¹⁹¹⁵ ₋₁₅₉₅	6.54	7.52
	sech	7.17 ^{+0.04} _{-0.04}	0.05	368 ⁺¹² ₋₁₀	2979 ⁺¹¹⁴⁵ ₋₉₅₅	6.39	7.26 ^{+0.02} _{-0.02}	0.07	371 ⁺⁷ ₋₅	2266 ⁺¹⁹⁵⁰ ₋₁₆₂₀	7.44	
	sech ²	6.99 ^{+0.03} _{-0.03}	0.06	442 ⁺¹⁰ ₋₁₀	1975 ⁺⁶¹⁰ ₋₃₈₀	7.30	7.05 ^{+0.02} _{-0.02}	0.09	469 ⁺⁷ ₋₇	1010 ⁺⁶²⁰ ₋₅₀₀	10.59	
(9,10]	exp	7.91 ^{+0.02} _{-0.02}	0.06	159 ⁺⁴ ₋₃	1520 ⁺⁵¹⁰ ₋₃₁₀	7.97	7.87 ^{+0.01} _{-0.01}	0.01	178 ⁺¹ ₋₁	1125 ⁺²⁷⁰ ₋₁₉₀	0.12	7.60
	sech	7.64 ^{+0.02} _{-0.02}	0.06	269 ⁺⁵ ₋₅	2695 ⁺⁹⁸⁰ ₋₇₅₅	7.42	7.58 ^{+0.01} _{-0.01}	0.01	295 ⁺² ₋₂	2382 ⁺⁸⁰⁰ ₋₆₉₅	0.11	
	sech ²	7.53 ^{+0.02} _{-0.02}	0.07	307 ⁺⁷ ₋₇	1680 ⁺⁵⁸⁰ ₋₃₄₅	10.72	7.42 ^{+0.01} _{-0.01}	0.02	358 ⁺³ ₋₃	1370 ⁺⁷⁰⁵ ₋₅₉₀	1.06	
(10,11]	exp	8.54 ^{+0.01} _{-0.01}	0.02	116 ⁺¹ ₋₁	2138 ⁺⁵⁶⁰ ₋₃₉₀	1.28	8.30 ^{+0.02} _{-0.02}	0.04	152 ⁺⁴ ₋₄	1065 ⁺⁸⁹⁰ ₋₇₄₅	7.94	7.73
	sech	8.25 ^{+0.01} _{-0.01}	0.02	192 ⁺² ₋₂	2447 ⁺⁷⁵⁰ ₋₄₅₀	2.23	8.04 ^{+0.02} _{-0.02}	0.03	245 ⁺⁷ ₋₅	1820 ⁺¹⁶⁸⁰ ₋₁₄₀₀	4.24	
	sech ²	8.10 ^{+0.01} _{-0.01}	0.02	229 ⁺² ₋₂	1704 ⁺³⁵⁰ ₋₂₄₀	1.23	7.96 ^{+0.01} _{-0.01}	0.01	281 ⁺³ ₋₃	2470 ⁺²⁰⁴⁰ ₋₁₇₀₀	1.30	
(11,12]	exp	7.61 ^{+0.01} _{-0.01}	0.01	155 ⁺² ₋₂	1755 ⁺⁹⁴⁰ ₋₄₈₀	0.01	8.05 ^{+0.01} _{-0.01}	0.01	125 ⁺¹ ₋₁	1920 ⁺¹⁰⁵⁰ ₋₈₇₅	0.13	7.91
	sech	7.39 ^{+0.01} _{-0.01}	0.01	242 ⁺³ ₋₃	2720 ⁺⁵⁶⁵ ₋₄₀₅	0.03	7.76 ^{+0.01} _{-0.01}	0.01	206 ⁺² ₋₂	1295 ⁺⁶⁶⁰ ₋₅₅₀	0.17	
	sech ²	7.34 ^{+0.01} _{-0.01}	0.01	264 ⁺¹ ₋₁	2985 ⁺¹⁵⁵ ₋₁₀₀	0.10	7.63 ^{+0.01} _{-0.01}	0.03	245 ⁺³ ₋₃	1800 ⁺¹⁴⁴⁵ ₋₁₂₀₅	0.94	

Table 5

Logarithmic solar space densities, n^* , for stars with absolute magnitudes $10 < M(g) \leq 11$ for six fields estimated by fitting the derived space densities with the Galactic disc model of Chen et al. (2001). The symbol s is the standard deviation. The local logarithmic solar space density of Hipparcos (Jahreiss & Wielen, 1997) is $\odot = 7.73$.

Field	n^*	s
F1	7.45	0.33
F2	7.49	0.37
F3	7.65	0.40
F4	7.52	0.37
F5	7.47	0.33
F6	7.65	0.33

Table 6

The scaleheight, H (pc), and scalelength, h (pc), as a function of both absolute magnitude and longitude for six fields.

$M(g) \rightarrow$		(8,9]			(9,10]			(10,11]			(11,12]		
Field	$l(^{\circ})$	n^*	H	h	n^*	H	h	n^*	H	h	n^*	H	h
F1	4.58	7.46	193	1967	7.60	229	1038	7.79	239	1022	7.74	121	2619
F2	15.93	7.45	203	1260	7.53	259	1030	7.84	253	1250	7.29	161	2703
F3	42.28	7.45	208	1281	7.64	269	2695	8.10	229	1704	7.61	155	1755
F4	61.62	7.44	220	1690	7.56	292	2313	7.85	275	1237	7.78	129	2448
F5	71.29	7.45	225	1606	7.52	285	1950	7.76	294	2804	7.72	134	1845
F6	83.38	7.55	226	2350	7.58	295	2382	7.96	281	2470	8.05	125	1920
Average			212	1692		272	1901		262	1748		138	2215

Table 7

Coefficients a_i and b_i ($i=0$ and 1) in the eqs. (8) and (9) and the squared correlation coefficient R^2 .

$M(g)$	$H = a_1(l) + a_0$			$h = b_1(l) + b_0$		
	a_1	a_0	R^2	b_1	b_0	R^2
(8, 9]	0.417	193.1	0.96	0.01	1.451	0.15
(9, 10]	0.750	236.6	0.89	0.02	1.100	0.57
(10, 11]	0.625	232.8	0.59	0.02	0.887	0.63
(11, 12]	-0.158	144.9	0.09	-0.01	2.654	0.49